Backscatter-Aided Hybrid Data Offloading for Wireless Powered Edge Sensor Networks

Yuze Zou*†, Jing Xu†, Shimin Gong‡, Yuanxiong Guo§, Dusit Niyato*, and Wenqing Cheng†
*School of Computer Science and Engineering, Nanyang Technological University, Singapore
†School of Electronic Information and Communications, Huazhong University of Science and Technology, China
‡School of Intelligent Systems Engineering, Sun Yat-sen University, China
§Department of Information Systems and Cyber Security, University of Texas at San Antonio, USA

***Abstract*—In this paper, we consider a backscatter-aided hybrid data offloading scheme for a batteryless wireless sensor network. All sensor devices on the edge are coordinated by a hybrid access point (HAP), while also provides power for them via wireless power transfer. Co-located with the HAP, an edge computing server is set up to provide the computation and caching capabilities for the edge devices with insufficient power and computation resources. Each node is allocated a fixed time-slot for data offloading via either the conventional active communications or the passive backscatter communications. Such a hybrid data offloading scheme can flexibly control the trade-off between power consumption and data rate in offloading. We aim to minimize the total energy consumption by optimizing the offloading strategy of each edge device and the HAP's wireless power allocation over different edge devices. We show that the energy minimization problem exhibits a convex reformulation. For practical consideration, we devise a distributed algorithm to solve the problem. The numerical results demonstrate that the distributed algorithm can achieve a near-optimal performance. With a fixed transmit power at the HAP, our proposed hybrid offloading scheme provides a higher offloading throughput compared to the state-of-the-art data offloading schemes.**

I. Introduction

The future wireless networks are anticipated to connect billions of devices such as wearable electronics, wireless sensors, and handhold devices [1]. We expect to embrace a dramatic traffic increase in machine-to-machine communications, which provides the cyber-physical infrastructure involving persistent information gathering, processing, and communications [2]. Currently, it is still challenging to provide these devices with enhanced computation capability in an economic way, especially for low-cost and low-power sensor devices. To this end, edge computing has emerged as a promising technique by providing cloud-like computation capability closer to numerous wireless devices, referred to as the edge devices.

The work of Shimin Gong was supported in part by National Science Foundation of China (NSFC) under Grant 61601449, 61972434, and the Shenzhen Talent Peacock Plan Program under Grant KQTD2015071715073798. The work of Dusit Niyato was supported in part by A*STAR-NTU-SUTD Joint Research Grant Call on Artificial Intelligence for the Future of Manufacturing RGANS1906, WASP/NTU M4082187 (4080), Singapore MOE Tier 1 under Grant 2017-T1-002-007 RG122/17, MOE Tier 2 under Grant MOE2014-T2-2-015 ARC4/15, Singapore NRF2015-NRF-ISF001-2277, and Singapore EMA Energy Resilience under Grant NRF2017EWT-EP003-041. Corresponding author: Shiming Gong.

The edge computing server can be integrated with the wireless access points or small-cell base stations, e.g., [3] and [4]. The edge devices can offload their sensed data and computations (e.g., data encoding, compressing, and encryption) to the computing server with more powerful computation capability. Then, the computing server returns the processed data to the edge devices. As such, computation offloading can facilitate real-time processing of the computation-intensive tasks at the low-power edge devices. Data offloading reduces the power consumption of edge devices spent on data processing. Whereas data offloading itself via wireless communications is inherently power consuming by using conventional radio architecture [5], referred to as the active radio. Due to prevailing use of power consuming components, e.g., power amplifier and analogy/digital converter, the active radio's power consumption can be hardly reduced without compromising the transmission performance. The high power consumption in wireless communications may not be affordable by low-power sensor devices and hence prevent them from using edge computing. Though RF-based wireless power transfer can supply power for wireless devices [6], the power supply from RF energy harvesting is typically very low to sustain active communications [7].

Recently, the wireless backscatter communications technique is introduced to bridge the gap between power demand in wireless transmissions and power supply from energy harvesting. The backscatter radios operate in *passive* mode by modulating and reflecting the incident RF signal via the change of load impedance [8]. Without using power-consuming components, the passive radio consumes orders of magnitude less power than an active radio, making wireless power transfer a feasible solution to sustain wireless backscatter communications. The passive radios are featured with low power consumption, low data rate, and vulnerable to the channel variations [9]. Whereas the active radios can transmit more reliably with a higher data rate by adapting the transmit power against the channel fading effect. We expect to achieve a radio diversity gain by switching data offloading in two radio modes [10]. The authors in [11] and [12] showed that the integration of backscatter radios with a cognitive radio network can significantly improve the overall network performance, by allowing the secondary users to flexibly

978-1-7281-0962-6/19/$31.00 ©2019 IEEE

transit among the states of energy harvesting, passive and active communications.

In this paper, we consider a hybrid data offloading scheme combining passive and active communications in a wireless powered edge computing scenario. All edge devices are wirelessly powered by RF signals from a hybrid access point (HAP) co-located with a computing server. If one edge device has low workload, we can employ backscatter communications to reduce the power consumption at the edge device. When the workload is high, we resort to active communications to speed up task offloading. This allows us to better control the trade-off between the power consumption and transmission rate in data offloading. Considering the channel variations and different workload, we aim to minimize the total energy consumption of the system by optimizing the offloading strategy of each edge device and the HAP's power allocation over different edge devices. A distributed solution is proposed to iterate between two sub-problems: the HAP's power allocation and the offloading scheduling at individual edge devices. To the best of our knowledge, we are the first to consider backscatter-aided hybrid offloading scheme in mobile edge computing. Our numerical results demonstrate that the hybrid offloading scheme can accommodate more workload given a fixed amount of energy at the HAP.

II. System Model

We consider a wireless edge sensor network consisting of N sensor nodes powered by one HAP, which integrates the computing server with powerful computing and caching resources, as depicted in Fig. 1. Let $\mathcal{N} = \{1, 2, ..., N\}$ denote the index set of all edge nodes and S_i denote the i-th edge node, for $i \in \mathcal{N}$. The edge nodes are deployed to collect and send back the data to back-end server through the HAP. We can envision the edge nodes as wearable devices that constantly monitor health-related signals or location information. The sensing information can be analysed locally or remotely by machine learning algorithms for classification, prediction, and decision-making. Due to limited energy supply and a large amount of data, the edge nodes are motivated to offload their data and computation to the edge computing server for more efficient processing. Each device is equipped with a single antenna capable of harvesting energy from the single-antenna HAP. The complex uplink and downlink channels between HAP and S_i are denoted by $h_i \in \mathcal{C}$ and $g_i \in \mathcal{C}$, respectively. The HAP schedules the data transmission of each node in a time-division multiple access (TDMA) model. Each S_i is allocated a time slot for its data offloading and can harvest energy in other time slots. In the time slot t_i, node S_i collects L_i bits of data (denoted as the workload) to be processed either locally or remotely at the computing server.

A. Hybrid Data Offloading Scheme

The data offloading from each edge node to the computing server can be performed in either passive or active communications mode, depending on its energy profile and the channel conditions. The switch between the passive and active mode can be achieved by tuning the load impedance, e.g., [5] and [13]. In passive mode, the HAP's beamforming provides the carrier signal for the edge node to perform backscatter communications. A part of the incident RF signal is reflected back and the other part is still captured by the antenna and converted to direct current power. Given a varying load impedance, the RF signal reflected into air has different power levels that can be detected and demodulated at the computing server. In the active mode, the load impedance of the edge node matches to its antenna impedance, maximizing the antenna efficiency in active data communications. Note that the energy for the active communications of one edge node is harvested in other time slots. By allowing radio mode switching, we further divide each time slot t_j into two sub-slots as shown in Fig. 1(b). Namely, one sub-slot $t_{a,j}$ is used for data offloading in the active mode and the other sub-slot $t_{p,j}$ is for backscatter communications. The active data offloading is powered by the energy harvested from the HAP over consecutive time slots. In the passive data offloading, a part of the incident RF signals, denoted by the power splitting parameter ρ_j, is harvested to power the backscatter radio, and the other part $1-\rho_j$ is modulated and instantly reflected back to the HAP.

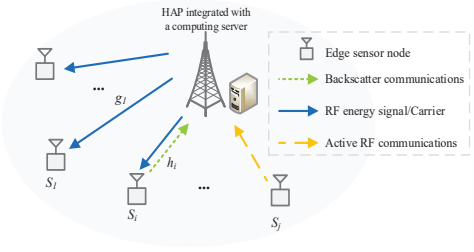

(a) Data offloading in wireless powered sensor network

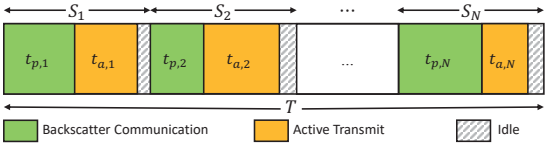

(b) Hybrid data offloading

Fig. 1. Backscatter-aided hybrid data offloading for wireless sensor network.

B. Signal Model

Let $p_{a,i}$ denote the transmit power in active data offloading. The received signal at HAP is given by $y = \sqrt{p_{a,i}} h_i s(t) + \nu_d$, where $s(t)$ denotes the information of S_i with unit power, and $\nu_d \sim \mathcal{CN}(0, \sigma^2)$ denotes the noise at the HAP, which follows complex Gaussian distribution with zero mean and σ^2 variance. Then, the normalized data rate in the active mode can be represented by

$$r_{a,i} = B \log_2 \left(1 + p_{a,i} |h_i|^2 / \sigma^2\right), \tag{1}$$

where B denotes the bandwidth of active data transmission. The relationship between $p_{a,i}$ and $r_{a,i}$ is given by:

$$p_{a,i} = \beta(r_{a,i}) \triangleq \left(2^{r_{a,i}/B} - 1\right) \sigma^2 / |h_i|^2. \tag{2}$$

Hence, the total power consumption in active communications can be denoted by $\tilde{\beta}(r_{a,i}) \triangleq \beta(r_{a,i}) + p_{c,i}$, which includes $\beta(r_{a,i})$ for data transmission and a constant portion $p_{c,i}$ for powering the circuit. For passive data offloading, the data rate can be viewed as a constant, i.e., $r_{p,i} = r_p$, which relates to the channel dynamics and the signal detection schemes at the receiver [9]. By the power splitting scheme, a part ρ_i of the incident RF power will be harvested as energy to power the circuit of backscatter radio [11].

III. Energy Minimization for Hybrid Data Offloading

Note that all batteryless edge devices are powered by the HAP via wireless power transfer and RF-based energy harvesting. Hence, we aim to minimize the HAP's energy consumption while satisfying the data offloading requests from all the edge devices. The total energy consumption of HAP can be simply denoted as $\sum_{i\in\mathcal{N}} p_0 t_{p,i}$, as it only provides carrier signals for backscatter communications during the sub-slot $t_{p,i}$, while keeping silence when edge devices transmit in active mode during the sub-slot $t_{a,i}$. Without loss of generality, we omit the power consumption in computation, as it only relates to the workload instead of the data offloading strategy. Let $\boldsymbol{l}_a \triangleq [l_{a,1}, ..., l_{a,N}]^T$ and $\boldsymbol{l}_b \triangleq [l_{b,1}, ..., l_{b,N}]^T$ denote workload of individual node offloaded to the HAP via active and backscatter communications, respectively. The energy minimization can be formulated as follows:

$$\min_{\boldsymbol{t}_a, \boldsymbol{t}_p} \quad \sum_{i\in\mathcal{N}} p_0 t_{p,i} \tag{3a}$$

$$\text{s.t} \quad t_{a,i} + t_{p,i} \le T/N, \quad \forall i \in \mathcal{N} \tag{3b}$$

$$l_{a,i} + l_{p,i} \ge L_i, \quad \forall i \in \mathcal{N} \tag{3c}$$

$$t_{a,i}\tilde{\beta}\left(\frac{l_{a,i}}{t_{a,i}}\right) \le \eta \sum_{j\in\mathcal{N}_i} p_0 g_i^2 t_{p,j}, \forall i \in \mathcal{N} \tag{3d}$$

$$\boldsymbol{t}_a \succeq 0, \boldsymbol{t}_p \succeq 0, \boldsymbol{l}_a \succeq 0, \tag{3e}$$

where $\boldsymbol{t}_p \triangleq [t_{p,1}, t_{p,2}, ..., t_{p,N}]^T$ and $\boldsymbol{t}_a \triangleq [t_{a,1}, ..., t_{a,N}]^T$ denote the data offloading time in passive and active mode, respectively, for each node. The downlink channel g_i for wireless power transfer determines the amount of energy that can be harvested by the edge node S_i on all other time slots $j \in \mathcal{N}_i \triangleq \mathcal{N} \setminus \{i\}$. The constraint (3b) denotes the time allocation for all nodes. The constraint (3c) ensures that all workload can be offloaded to the computing server for processing. The constraint (3d) denotes the power budget of each edge node when it transmits in active mode. Although problem (3) can be solved efficiently by a centralized algorithm, it requires information from all edge nodes, including channel state information and workload. This increases the communication overhead and processing delay. In the sequel, we are motivated to develop a distributed algorithm that is more amenable for practical implementation.

Note that different edge nodes are coupled through the energy harvesting constraint in (3d). To solve the optimization problem (3), we decompose it to sub-problems with reduced complexity that can be solved locally by an individual edge node. By overhearing the channel and harvesting RF power, each edge node can be aware of its energy supply in the RHS of constraint (3d). For simplicity, we denote the energy supply of S_i as $E_i \triangleq \eta \sum_{j\neq i} p_0 g_i^2 t_{p,j}$. Hence, for any edge device S_i, the optimal data offloading strategy can be updated by solving the following optimization problem locally:

$$\min_{t_a, t_p, r_a} \quad t_p \tag{4a}$$

$$\text{s.t} \quad t_a + t_p \le t \text{ and } t_a r_a + t_p r_p \ge L \tag{4b}$$

$$t_a \beta(r_a) + p_c t_a \le E \tag{4c}$$

$$r_{\min} \le r_a \le r_{\max} \tag{4d}$$

$$t_a \ge 0, t_p \ge 0. \tag{4e}$$

The subscript is omitted for notational convenience. The constraint (4d) means that the data rate r_a in active mode is confined in the range $[r_{\min}, r_{\max}]$, which depends on the workload and channel conditions. We assume $r > r_{\min} \triangleq L/t$ to ensure that the edge node can complete offloading the workload L before the end of one time slot. The maximum $r_{\max}$ is limited by the transmit power of the edge node and thus by its energy supply E. As the HAP's transmit power is fixed, we only need to minimize the time t_p for the backscatter communications. At the beginning of each sub-slot, the edge node solves problem (4) according to its workload L and the energy supply E. Then, the optimal time t_p, as well as the workload will be sent to the HAP via data offloading.

A. Hybrid Data Offloading at Individual Edge Node

In the sequel, we aim to find a closed-form solution of problem (4) to minimize the computation at individual edge nodes. To proceed, we find that problem (4) is determined by three variables (t_a, t_p, r_a), and we can further divide its solution into two sub-procedures: With fixed r_a, we can first determine the optimal solution (t_a, t_p) and then minimize the objective with respect to r_a. Given any $r_a \in [r_{\min}, r_{\max}]$, problem (4) becomes a linear program and thus we can easily retrieve the upper bound (the maximum feasible value) of t_a, denoted by $t_a^{\max}(r_a)$, at one intersection point of the inequalities in (4b)-(4e). The feasible region with fixed r_a is illustrated in Fig. 2. Hence, the maximum $t_a^{\max}$ is given by

$$t_a^{\max}(r_a, E) = \frac{E}{\beta(r_a) + p_c}, \tag{5}$$

which depends on r_a and the energy supply E. It is obvious that $t_a^{\max}$ becomes larger with the increase of energy E.

We consider a practical assumption $r_p t < L < r_a t$ or $L/r_p > t > L/r_a$. This implies that the data rate in active mode is larger than that of backscatter communications. Moreover, if energy supply E is sufficient, each edge node can complete offloading its workload to the HAP via active data transmissions. Based on above assumption and the geometric

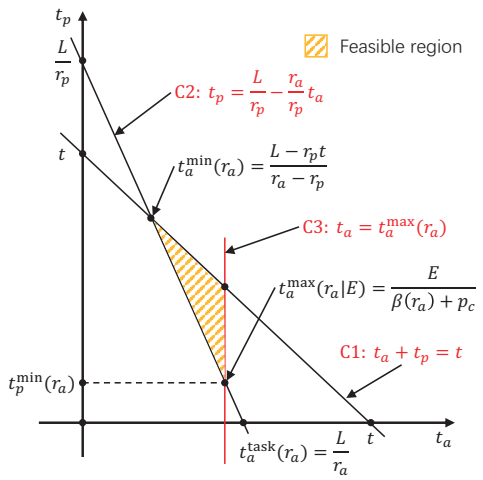

Fig. 2. Feasible region of individuals' offloading optimization with fixed r_a.

interpretation in Fig. 2, we can easily determine the minimum $t_p^{\min}(r_a)$ as a function of the data rate r_a in active mode:

$$t_p^{\min}(r_a) = \begin{cases} 0, & \frac{E}{\beta(r_a)+p_c} \geq \frac{L}{r_a} \\ \frac{L}{r_p} - \frac{r_a}{r_p}\frac{E}{\beta(r_a)+p_c}, & \frac{E}{\beta(r_a)+p_c} \in \left[\frac{L-r_p t}{r_a - r_p}, \frac{L}{r_a}\right) \end{cases}. \tag{6}$$

For the third case $\frac{E}{\beta(r_a)+p_c} < \frac{L-r_p t}{r_a - r_p}$, the edge node is unable to offload its workload with one time slot due to insufficient energy supply E. In the sequel, we discuss over two feasible cases in (6) and determine the optimal solution in each case.

We first check the feasibility of two cases in (6). This allows us to pick the correct case to calculate $t_p^{\min}$. The feasibility check amounts to find solutions to the following equations:

$$\beta(r_a) + p_c = r_a E/L, \tag{7a}$$
$$\beta(r_a) + p_c = (r_a - r_p)E/(L - r_p t). \tag{7b}$$

It is easy to observe that (7a) and (7b) admits the same form $\beta(r_a) = a_i r_a + b_i$, with $i = 1$ and $i = 2$ corresponding to (7a) and (7b), respectively, and (a_i, b_i) given as follows:

$$\begin{cases} a_1 = \frac{Eh^2 B}{L\sigma^2} \\ b_1 = 1 - \frac{p_c h^2}{\sigma^2} \end{cases}, \text{ and } \begin{cases} a_2 = \frac{Eh^2 B}{(L - r_p t)\sigma^2} \\ b_2 = \left(1 - \frac{p_c h^2}{\sigma^2}\right) - \frac{Eh^2 r_p}{(L - r_p t)\sigma^2} \end{cases}.$$

Proposition 1. *The solutions to* (7)*, if exist, are given by*

$$\begin{cases} r_{i,1} &= -\frac{B}{\ln 2} W_0\left(-\frac{\ln 2}{a_i} 2^{-\frac{b_i}{a_i}}\right) - \frac{b_i}{a_i} B \\ r_{i,2} &= -\frac{B}{\ln 2} W_{-1}\left(-\frac{\ln 2}{a_i} 2^{-\frac{b_i}{a_i}}\right) - \frac{b_i}{a_i} B \end{cases} \tag{8}$$

where $r_{i,1} \leq r_{i,2}$*,* $W_0(x)$ *and* $W_{-1}(x)$ *represents two branches of Lambert W function [14], respectively.*

The proof is given in Appendix A. By comparing r_a to the zero points $r_{i,1}$ and $r_{i,2}$, we can evaluate $t_p^{\min}$ either on the first case or the second case in (6). In particular, if $r_a \in [r_{i,1}, r_{i,2}]$, then $\beta(r_a) \leq a_i r_a + b_i$, otherwise $\beta(r_a) > a_i r_a + b_i$. As $t_p^{\min}$ equals to trivial zero as shown in the first case of (6), we can focus on the second case and determine the optimal r_a^* by the following proposition.

Proposition 2. *The optimal* r_a^* *is given by*

$$r_a^* = \frac{B}{\ln 2}\left(W_0\left(\frac{p_c h^2/\sigma^2 - 1}{e}\right) + 1\right) \tag{9}$$

The proof is given in Appendix B. Till this point, we can detail the distributed solution procedure for (4) in Algorithm 1. It firstly retrieves the zero points to equation (6) by Proposition 1, and then check the feasibility sequentially. For notational convenience, we define $t_p^* \triangleq \min_{r_a \in [r_{\min}, r_{\max}]} t_p^{\min}(r_a)$ as the optimum of t_p and $\overline{[r_{1,1}, r_{1,2}]} \triangleq (-\infty, r_{1,1}) \cup (r_{1,2}, +\infty)$ as the complementary set of $[r_{1,1}, r_{1,2}]$. Note that $[r_{1,1}, r_{1,2}]$ will be an empty set if $r_{1,1}$ and $r_{1,2}$ have no real solutions.

Due to the coupling between differen edge nodes, referred to as the energy budget constraint in (3d), individual node's update on offloading strategy will change the energy supply of other nodes. Hence, each edge nodes has to take turns to update the offloading strategy by solving problem (4) locally.

Algorithm 1 Distributed Algorithm for Hybrid Offloading

Input: Energy supply E and workload L of each node
Output: Transmission time (t_p, t_a) and active data rate r_a
  Retrieve $(r_{1,1}, r_{1,2})$ and $(r_{2,1}, r_{2,2})$ by Proposition 1
  Retrieve r_a^* by Proposition 2
  if $[r_{1,1}, r_{1,2}] \cap [r_{\min}, r_{\max}] \neq \emptyset$ **then**
    $t_p^* \leftarrow 0$,
  else if $[r_{2,1}, r_{2,2}] \cap [r_{\min}, r_{\max}] = \emptyset$ **then**
    Solve t_p^* to maximize the workload
  else if $\overline{[r_{1,1}, r_{1,2}]} \cap [r_{2,1}, r_{2,2}] = \emptyset$ **then**
    Solve t_p^* to maximize the workload
  else if $r_a^* \in \overline{[r_{1,1}, r_{1,2}]} \cap [r_{2,1}, r_{2,2}]$ **then**
    $t_p^* \leftarrow \frac{L}{r_p} - \frac{r_a^*}{r_p}\frac{E}{\beta(r_a^*)+p_c}$,
  else
    $t_p^* \leftarrow \min_{i,j \in \{1,2\}} \left\{\frac{L}{r_p} - \frac{r_{i,j}}{r_p}\frac{E}{\beta(r_{i,j})+p_c}\right\}$.
  end if

IV. Numerical Results

In this section, we compare the performance of our hybrid data offloading scheme (denoted as Hybrid-DOS) with the conventional active offloading scheme without the support for backscatter communications (denoted as Active-DOS). Besides, centralized and distributed algorithms for hybrid data offloading (denoted as Cent-HOS and Dist-HOS, respectively) are compared as well. We set a fixed transmit power at HAP by $p_t = 100$ mW. The frame length is set by $T = 10$, equally shared by $N = 10$ edge devices. We also assume that each edge node will not carry out local computation and all workload has to be offloaded to the computing server via either active or passive communications. For simplicity, we assume that each edge node has the same workload $L = 10$ kbits, unless otherwise specified. As all workload has been processed at the computing server, the power consumption in computation can be viewed as constant and hence we only focus on the HAP's energy consumption in wireless power transfer. The energy conversion efficiency is set as η = 0.8, and the constant circuit power at each edge node is $p_c = 1$ μW. We

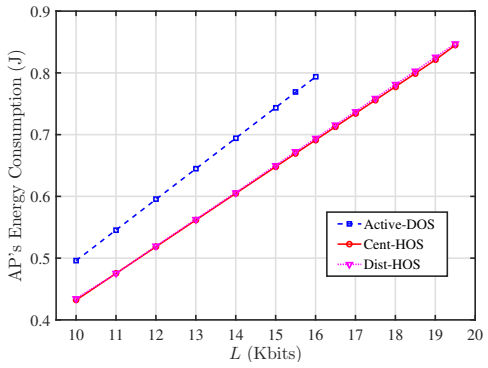

(a) The HAP's energy consumption

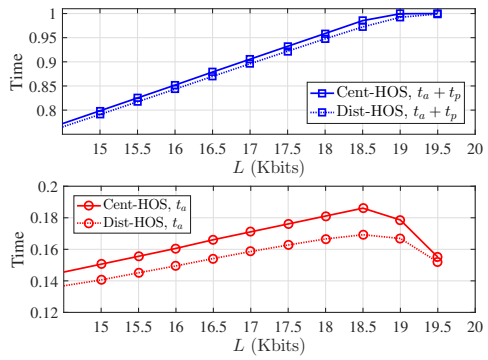

(b) Transmit time allocation

Fig. 3. The HAP's energy consumption and transmit time allocation.

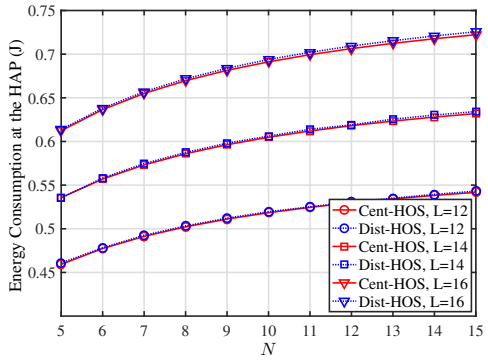

(a) Energy consumption at the HAP

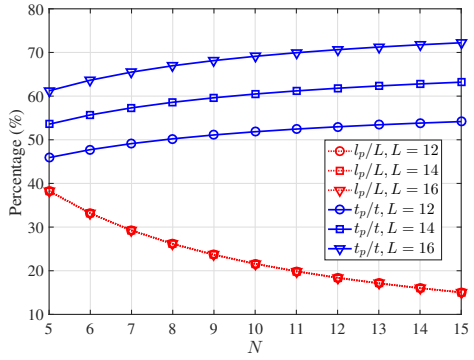

(b) Workload and transmit time of passive data offloading

Fig. 4. Energy consumption and individual nodes' offloading scheduling.

assume that constant data rate in passive mode is r_p = 5 kbps. The channel coefficients are fixed during one data frame. We set the downlink channel gain as $|g|^2 = -53$ dB and the uplink offloading channel gain as $|h|^2$ = -60 dB. The noise power is set to $\sigma^2 = -70$ dBm and the bandwidth is given by $B = 400$ kHz.

A. Throughput Performance with Different Workload

Fig. 3 shows the HAP's energy consumption and transmit time allocation with different workload at individual edge ndoes. We can observe that the Hybrid-DOS induces less power consumptions at the HAP compared to the Active-DOS. Moreover, the Hybrid-DOS is capable of offloading more workload than that of the Active-DOS. The maximum workload can be offloaded to the HAP via the Active-DOS is limited by 16 kbits while the Hybrid-DOS can offload a maximum of 19.5 kbits workload under the same settings. By optimizing the transmission scheduling in two modes, the Hybrid-DOS is more energy-efficient than the conventional Active-DOS. As the workload increases, we observe a linear increase in the HAP's energy consumption as shown in Fig. 3(a). Meanwhile, the time for data offloading, i.e., $t_a + t_p$ firstly increases lineally and then converges to the maximum (unit one in this case), as shown in Fig. 3(b). It is worth mentioning that t_a firstly increases with L then decreases as L is larger than 18.5 kbits. The reason is that, when workload is relatively small (i.e., $L < 18.5$ kbits), the energy requirement for active transmission is easy to fulfill as shown in Fig. 3(b), we have $t_a + t_p < 1$ when $L < 18.5$ kbits. However, when workload is large, the energy requirement becomes critical and more time is allocated for energy harvesting. Thus, we observe that t_p increases and t_a decreases accordingly. This verifies the benefit of complement data offloading via active and backscatter communications in Hybrid-DOS. Moreover, as shown in Fig. 3(a), the Dist-HOS can achieve nearly the same performance as that of Cent-HOS in terms of energy consumption at the HAP, which corroborates the effectiveness of the proposed distributed algorithm.

B. Throughput Performance with More Edge Nodes

In Fig. 4, we increase the number of edge nodes N from 5 to 15 and set the workload $L \in \{12, 14, 16\}$ kbits. As shown in Fig. 4(a), with a fixed number of edge nodes, the HAP consumes more energy with larger workload, which is consistent with the result shown in Fig. 3(a). The Dist-HOS and Cent-HOS have nearly the same performance as well. The HAP's energy consumption increases sub-linearly with the increase of N. In particular, with $L = 16$ kbits, the HAP's energy consumption is 0.73 J at $N = 15$ while 0.61 J at $N = 5$. Only 19.67% increase in the HAP's energy consumption to empower 10 more nodes to offload their workload. With more sensors in the network, there will be more opportunities for individual nodes to harvest energy.

Fig. 4(b) presents a more interesting result. It shows relative workload and transmit time for data offloading via backscatter communications with the Cent-HOS, respectively. For more edge nodes, the time allocation $t \triangleq T/N$ for each node will

correspondingly decrease. With fixed N, the relative transmit time (i.e., t_p/t) in passive mode will increase with a larger workload L. This is consistent with the result in Fig. 4(a) as the HAP consumes more energy consumption to emit carrier signals for backscatter communications. Moreover, the relative workload offloaded via backscatter communications (i.e., l_p/L) decreases with more edge nodes. This is also reasonable since each edge node can harvest more energy from others in this case. Hence, the active transmission will take more responsibility for data offloading in order to reduce the energy consumption at the HAP.

V. Conclusion

In this paper, we propose a hybrid offloading scheme for wireless powered edge computing, which integrates active and backscatter communications and exploits the radio's diversity gain. The hybrid scheme can balance energy consumption and data offloading rate by scheduling the transmission in two radio modes. A convex problem is formulated to minimize the energy consumption at the edge computing center. Afterwards, for practical implementation with reduced overhead, we devise a near-optimal distributed algorithm that requires each edge node to locally optimize its offloading strategy. Numerical results reveal that the proposed hybrid scheme outperforms the conventional active data offloading scheme. In the future, we will further discuss the hybrid offloading scheme under the scenario with multiple-antenna HAP and more flexible time allocation strategy, which can provide more optimization dimensions.

Appendix

A. Proof of Proposition 1

The equation $p^x = ax + b$ can be transformed via the substitution $-t = x + \frac{b}{a}$ into $tp^t = R = -\frac{1}{a}p^{-\frac{b}{a}}$, then we have, $t = \frac{W(R\ln p)}{\ln p}$, which yields the solution $x = -\frac{W(-\frac{\ln p}{a}p^{-\frac{b}{a}})}{\ln p} - \frac{b}{a}$. Moreover, the Lambert W function $W(x)$ represents the solutions y of the equation $ye^y = x$ for any complex number x, which has following properties [14]:

- For $x < -\frac{1}{e}$, there are no real solution.
- For all real x in the range $-\frac{1}{e} < x < 0$, there are exactly two distinct real solutions. The larger one is represented by $w = W_0(x)$, and the smaller one is represented by $w = W_{-1}(x)$.
- For $x = -\frac{1}{e}$, there is exactly one real solution $W_0(-\frac{1}{e}) = W_{-1}(-\frac{1}{e}) = -1$.

Therefore, when $-\frac{\ln p}{a}p^{-\frac{b}{a}} \geq -\frac{1}{e}$, since $p > 1$ and $a > 0$, $-\frac{\ln p}{a}p^{-\frac{b}{a}} < 0$, then we can get two real solutions for $p^x = ax + b$, denoted by $x_1 = -\frac{W_0(-\frac{\ln p}{a}p^{-\frac{b}{a}})}{\ln p} - \frac{b}{a}$ and $x_2 = -\frac{W_{-1}(-\frac{\ln p}{a}p^{-\frac{b}{a}})}{\ln p} - \frac{b}{a}$, respectively. Note that $x_1 \leq x_2$. Besides, if $-\frac{\ln p}{a}p^{-\frac{b}{a}} < -\frac{1}{e}$, there exist no real solutions for $p^x = ax + b$, thus $p^x > ax + b$ for $\forall x \in (-\infty, +\infty)$.

B. Proof of Proposition 2

According to the second case in (6), the first-order derivative over r_a is given as follows:

$$\frac{\mathrm{d}t_p^{\min}}{\mathrm{d}r_a} = -\frac{E(\beta(r_a) - r_a\beta'(r_a) + p_c)}{r_p\left(\beta(r_a) + p_c\right)^2},$$

For notational convenient, we define $A(r_a) \triangleq \beta(r_a) - r_a\beta'(r_a) + p_c$ and $B(r_a) \triangleq r_p\left(\beta(r_a) + p_c\right)^2$. Then $\frac{\mathrm{d}t_p^{\min}}{\mathrm{d}r_a} = -E\frac{A(r_a)}{B(r_a)}$. In the sequel, the second-order derivative at r_a^* such that $A(r_a^*) = 0$ is given by

$$\left.\frac{\mathrm{d}^2 t_p^{\min}}{\mathrm{d}r_a^2}\right|_{r_a = r_a^*} = -E\frac{A'(r_a)}{B(r_a)} = \frac{Er_a\beta''(r_a)}{B(r_a)} > 0.$$

Therefore, r_a^* is the minimum point of $t_p^{\min}(r_a)$. To retrieve r_a^*, we need to solve $\beta(r_a) - r_a\beta'(r_a) + p_c = 0$. The solutions of it are given by (9) [15].

References

[1] M. Shafi, A. F. Molisch, P. J. Smith, T. Haustein, P. Zhu, P. D. Silva, F. Tufvesson, A. Benjebbour, and G. Wunder, "5G: A tutorial overview of standards, trials, challenges, deployment, and practice," *IEEE J. Sel. Area. Commun.*, vol. 35, no. 6, pp. 1201–1221, June 2017.

[2] R. Wang, J. Yan, D. Wu, H. Wang, and Q. Yang, "Knowledge-centric edge computing based on virtualized D2D communication systems," *IEEE Commun. Mag.*, vol. 56, no. 5, pp. 32–38, May 2018.

[3] Y. Mao, C. You, J. Zhang, K. Huang, and K. B. Letaief, "Mobile edge computing: Survey and research outlook." [Online]. Available: https://arxiv.org/abs/1701.01090v3

[4] S. Barbarossa, S. Sardellitti, and P. D. Lorenzo, "Communicating while computing: Distributed mobile cloud computing over 5G heterogeneous networks," *IEEE Signal Process. Mag.*, vol. 31, no. 6, pp. 45–55, Oct. 2014.

[5] J. Li, J. Xu, S. Gong, X. Huang, and P. Wang, "Robust radio mode selection in wirelessly powered communications with uncertain channel information," in *Proc. IEEE GLOBECOM*, Dec. 2017, pp. 1–6.

[6] D. Niyato, D. I. Kim, M. Maso, and Z. Han, "Wireless powered communication networks: Research directions and technological approaches," *IEEE Wireless Commun.*, vol. 24, no. 6, pp. 88–97, Dec. 2017.

[7] X. Lu, P. Wang, D. Niyato, D. I. Kim, and Z. Han, "Wireless networks with RF energy harvesting: A contemporary survey," *IEEE Commun. Surv. Tut.*, vol. 17, no. 2, pp. 757–789, 2015.

[8] C. Boyer and S. Roy, "Backscatter communication and RFID: Coding, energy, and MIMO analysis," *IEEE Trans. Commun.*, vol. 62, no. 3, pp. 770–785, Mar. 2014.

[9] V. Liu, A. Parks, V. Talla, S. Gollakota, D. Wetherall, and J. R. Smith, "Ambient backscatter: Wireless communication out of thin air," in *Proc. ACM SIGGOMM*, Aug. 2013, pp. 39–50.

[10] I. Veen, Q. Liu, P. Pawelczak, A. Parks, and J. R. Smith, "BLISP: Enhancing backscatter radio with active radio for computational RFIDs," in *proc. IEEE Int. Conf. RFID (RFID)*, May 2016, pp. 1–4.

[11] D. T. Hoang, D. Niyato, P. Wang, D. I. Kim, and Z. Han, "Ambient backscatter: A new approach to improve network performance for RF-powered cognitive radio networks," *IEEE Trans. Commun.*, vol. 65, no. 9, pp. 3659–3674, Sept. 2017.

[12] L. Xu, K. Zhu, R. Wang, and S. Gong, "Performance analysis of RF-powered cognitive radio networks with integrated ambient backscatter communications," *Wireless Commun. & Mobile Comput.*, pp. 1–16, 2018.

[13] J. Li, J. Xu, S. Gong, C. Li, and D. Niyato, "A game theoretic approach for backscatter-aided relay communications in hybrid radio networks," in *Proc. IEEE GLOBECOM*, Dec. 2018, pp. 1–6.

[14] R. M. Corless, G. H. Gonnet, D. E. Hare, D. J. Jeffrey, and D. E. Knuth, "On the lambertw function," *Adv. Comput. Math.*, vol. 5, no. 1, pp. 329–359, Dec. 1996.

[15] F. Wang, J. Xu, X. Wang, and S. Cui, "Joint offloading and computing optimization in wireless powered mobile-edge computing systems," in *Proc. IEEE ICC*, May. 2017, pp. 1–6.